Climate-controlled multidecadal variability in North African dust transport to the Mediterranean: Supplementary Information

Construction of ^{210}Pb age models

A series of 16 samples was taken at 3mm resolution from the core-top, to construct a ^{210}Pb activity profile. The samples were desalinated, then freeze-dried to estimate water content and dry bulk density. ^{210}Pb activity in 100mg of each sample was measured at the Royal Netherlands Institute for Sea Research (NIOZ) by α-spectrometry of its granddaughter ^{210}Po, which was precipitated on silver after digestion of the sample in an acid solution. A pair of alternative age models were established using the Constant Rate of Supply (CRS) and Constant Flux-Constant Sedimentation (CF-CS) approaches. The CRS model assumes a constant flux of ^{210}Pb to the sediment but calculates changes in the total sediment accumulation rate from deviations in the exponential decline of ^{210}Pb activity with depth. The CF-CS model assumes both the flux of ^{210}Pb and the total sediment accumulation rate to be constant and calculates an exponential best-fit of the data. See Boer et al. (2006) for full details of methodology.

ICP-MS data processing

Isotope specific LA-ICP-MS ion currents were corrected for inter-element ablation efficiency by calibrating to the external reference material NIST 610. All data was processed using the Lamtrace 2.16 software. The following oxides were assumed to sum to 100% of the total sediment material: $CaCO_3$, Na_2O, MgO, Al_2O_3, SiO_2, K_2O, MnO and Fe_2O_3. To correct for changes in ablation rate during scans- caused by variable proportions of resin in the ablated material- all major element data were initially calibrated to the counts of Si (mass 29) assuming a constant SiO_2 concentration. Variations from 100% in the subsequent oxide sum were then used to back-calculate major element compositional variability.

Controls on Total Dust Accumulation Rate

The total dust accumulation rate in the Atalante Basin was calculated by multiplication of total terrestrial oxide concentration and CRS-derived total mass accumulation rate at the 5mm resolution of the ^{210}Pb sampling scheme (Supplementary Fig. 1).

The dust accumulation rate shows a general decreasing trend from 1860 to the present day, onto which multidecadal variability is superimposed (Fig. 3B). The observed variability in dust composition might be expected to translate into a variable total dust flux to the basin, as the magnitude of the flux from different source regions varies. However, the two parameters are largely independent. The oscillations in total dust accumulation rate correspond to variability in PCA Axis 1, per definition independent of variability in PCA Axis 2 (Fig. 2B).

We suggest that processes within the water column and brine influence the total dust accumulation rate after deposition in the surface waters. Dust particles aggregate with biogenic material prior to sedimentation, hence changes in organic matter availability or composition may influence the efficiency of vertical transport to the seafloor (eg. Passow and de la Rocha, 2006), as may the strength of currents at different levels in the water column (Ratmeyer et al., 1999). The total accumulation rates at the coring site are also anomalously high for the Eastern Mediterranean (~0.0080 g cm^{-2} yr^{-1}

vs. ~0.0015 g cm^{-2} yr^{-1} in nearby non-brine core UM15, Rutten et al., 2000), due to focusing of material into accumulation centers within the basin. Hence, the variability in the total dust accumulation rate may also reflect changes in transport through the water column or the rate of focusing within the brine basin, both of which act to decouple total dust accumulation from climate variability.

Supplementary Figure captions

Supplementary Figure DR1. Calculation of dust accumulation rate (bottom) by multiplication of total terrestrial oxide concentration (top) and CRS-derived total mass accumulation rate (middle) at 5mm resolution of ^{210}Pb sampling scheme.

Supplementary Figure DR2. Persistent oscillations within the terrestrial component composition of NU15MC. Bottom: Extended LA-ICP-MS Mg/Al profile for full 40cm of NU15MC. Top: Mg/Al measured on discrete samples by ICP-OES on a parallel multicore. Solid black profile: 5-50cm bandpass filtered data to highlight oscillations and provide basis for inter-core correlation.

References Cited

Boer, W., van den Bergh, G.D., de Haas, H., de Stigter, H.C., Gieles, R., and van Weering, T.C.E., 2006, Validation of accumulation rates in Teluk Banten (Indonesia) from commonly applied Pb-210 models, using the 1883 Krakatau tephra as time marker: Marine Geology, v. 227, p. 263–277, doi: 10.1016/j.margeo.2005.12.002.

Ratmeyer, V., Fischer, G., Wefer, G., 1999, Lithogenic particle fluxes and grain size distributions in the deep ocean off northwest Africa: Implications for seasonal changes of aeolian dust input and downward transport, Deep-Sea Research (I) 46, 1289-1337.

Rutten, A., de Lange, G.J., Ziveri, P., Thomson, J., van Santvoort, P.J.M., Colley, S., and Corselli, C., 2000, Recent terrestrial and carbonate fluxes in the pelagic eastern Mediterranean; a comparison between sediment trap and surface sediment: Palaeogeography, Palaeoclimatology, Palaeoecology, v. 158, p. 197–213, doi: 10.1016/S0031-0182(00)00050-X.

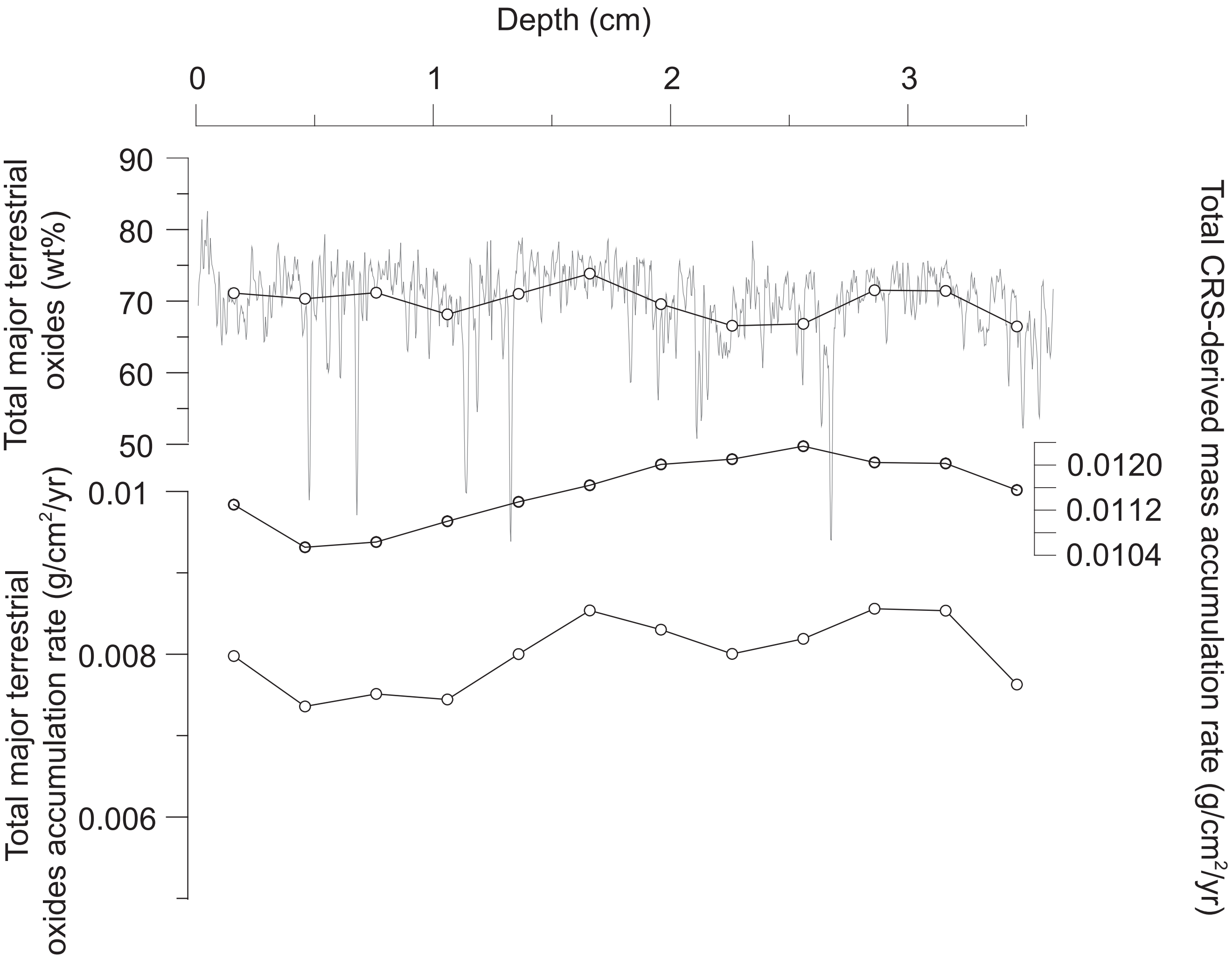
Depth (cm)
0
1
2
3
Total major terrestrial oxides (wt%)
90
80
70
60
50
Total major terrestrial oxides accumulation rate (g/cm^2/yr)
0.01
0.008
0.006
Total CRS-derived mass accumulation rate (g/cm^2/yr)
0.0120
0.0112
0.0104

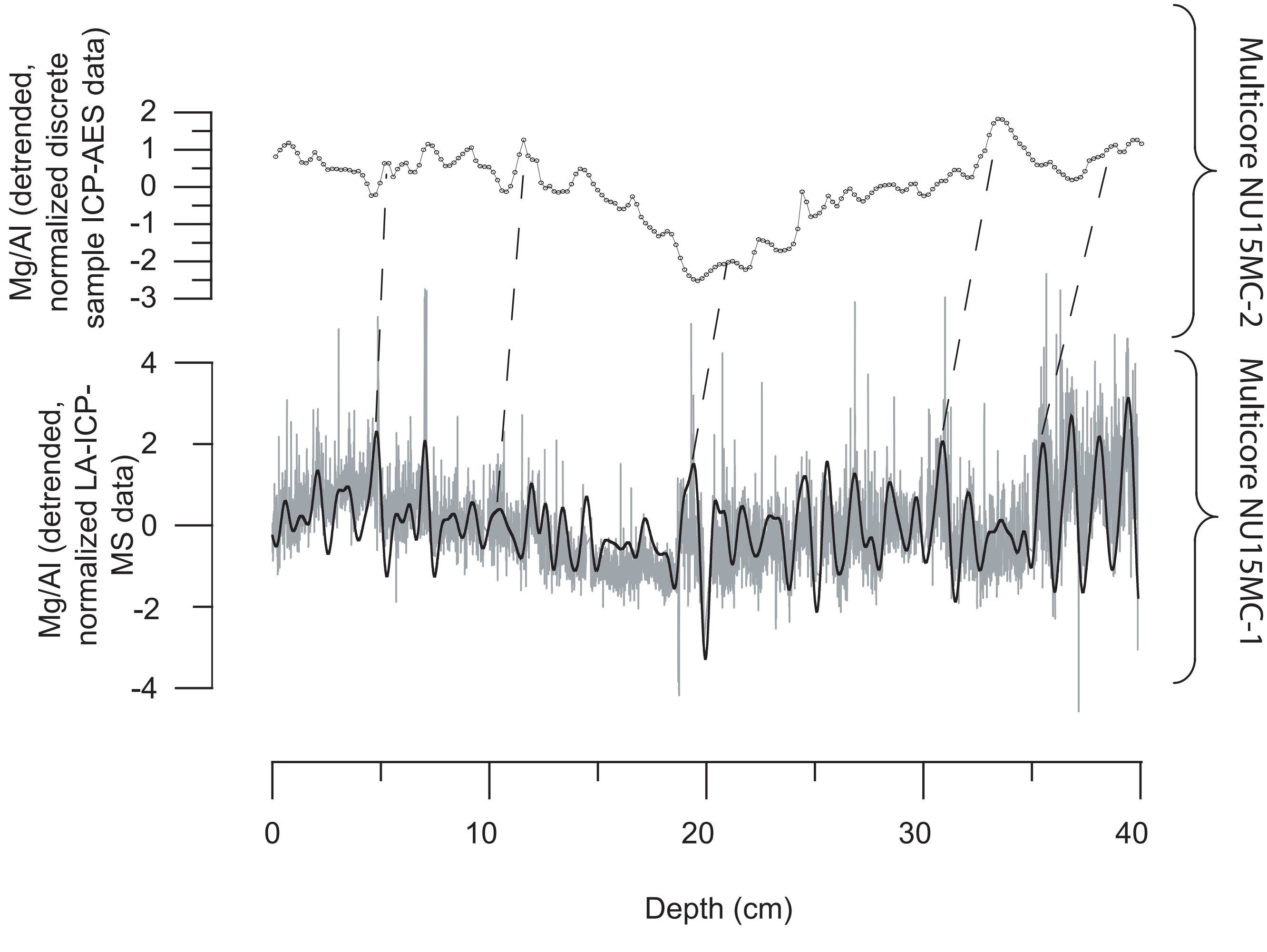

Mg/Al (detrended, normalized discrete sample ICP-AES data)
2
1
0
-1
-2
-3
Mg/Al (detrended, normalized LA-ICP-MS data)
4
2
0
-2
-4
0
10
20
30
40
Depth (cm)
Multicore NU15MC-2
Multicore NU15MC-1